ON THE ROLE OF SHEAR TRANSFER MECHANISMS IN THE LONGITUDINAL TENSILE FAILURE OF CFRP COMPOSITES

Gianmaria Bullegas[1], Silvestre T Pinho[1], Soraia Pimenta[2]

[1]Dept. of Aeronautics, Imperial College London, SW7 2AZ, London, UK
Email: silvestre.pinho@imperial.ac.uk, Web Page: wwwf.imperial.ac.uk/aeronautics/research/pinholab
[2]Dept. of Mechanical Engineering, Imperial College London, SW7 2AZ, London, UK
Email: soraia.pimenta@imperial.ac.uk, Web Page: www.imperial.ac.uk/people/soraia.pimenta

Keywords: CFRP, Longitudinal Tensile Failure, Size Effects, Fibre Bundle Model, Shear-lag

Abstract

A three-Dimensional (3D) Fibre Bundle Model (FBM) has been developed to simulate the longitudinal tensile failure and predict the statistical strength distribution of CFRP bundles of different sizes. An original semi-analytical approach has been developed to determine the stress field inside the bundle and predict the evolution of the failure process. The present model can account for the effects of fibre-matrix debonding, as well as the effect of the size of the cluster of broken fibres on the stress recovery length and, in turn, on the bundle strength. The model results compare favourably with different sets of experimental results, thus demonstrating the suitability of the modelling approach and the importance of including the previously mentioned effects in FBMs.

1. Introduction

The longitudinal tensile strength of Carbon Fibre Reinforced Plastics (CFRP) composite bundles is characterised by size effects related to both the number of fibres in the bundle and the bundle length [1–3]. This is due to the stochastic variability of the strength of single fibres. Being able to correctly model the failure process and predict these size effects on the bundle strength is fundamental for material development and structural design with composites. However, no modelling strategy has been universally accepted yet.

In a bundle of parallel fibres under longitudinal tensile load, the tensile stress in the bundle cross-section is uniform and equal to the asymptotic stress σ_∞, until the weakest fibre breaks. Once this happens, the load previously carried by the broken fibre is redistributed over the surviving fibres, creating a stress concentration and a non-uniform stress field.

The difference in tensile stress leads to the development of shear stresses in the matrix between the broken fibre and its neighbours. The matrix can then undergo plasticity or the matrix-fibre interface can fracture. In the former case, the value of the shear stress is equal to the yielding strength of the matrix; in the latter, it is equal to the friction stress acting at the fibre-matrix debonded interface. Due to the shear stress acting on its lateral surface, the broken fibre recovers the asymptotic stress σ_∞ over the recovery length ℓ_r, which determines the region of influence of the stress concentrations. These stress concentrations can induce further fibre breaks, eventually generating an avalanche effect, and thereby

Excerpt from ISBN 978-3-00-053387-7

forming clusters of broken fibres.

Several Fibre Bundle Models (FBMs) have been developed and are reported in the literature [3–13]. Most modelling approaches focused in detail on the stress redistribution and resulting stress concentration due to a single fibre break or a cluster of broken fibres in the 2D cross-section of the bundle [4, 6, 8, 10–12]. Comparatively less attention has been given to the shear transfer mechanisms and the effects of the stress recovery along the fibre direction.

FBMs for CFRP bundles typically assume perfect adhesion of the fibre-matrix interface, although different material behaviours (e.g. linear-elastic, elastic-plastic, perfectly plastic) for the matrix are considered [4, 6, 12]. However, fracture of the fibre-matrix interface has been observed experimentally [14], and this effect can strongly influence the stress recovery length of the broken fibres.

FBMs which directly calculate the 3D stress state for a given configuration of broken fibres in the bundles are usually capable of capturing the dependency of the stress recovery length on the size of the cluster of broken fibres [4]. FBMs which calculate the 3D stress state using superposition algorithms [5, 8, 12] typically tend to neglect this effect, and calculate the stress profile along the broken fibres in the recovery length using an analytical shear-lag function, considering a shear-lag perimeter which is equivalent to the single fibre circumference.

Pimenta and Pinho [13] recently developed a Hierarchical Fibre Bundle Model (HFBM) which accounts for the variation of the recovery length with the size of the cluster of broken fibres. This analytical model is computationally efficient as it models the failure process statistically, rather than simulating explicitly each fibre break.

Therefore, there is great interest for a 3D FBM which can explicitly simulate the failure process of CFRP bundles, and allows to investigate the role of the longitudinal shear transfer mechanisms: in particular, the effect of fibre matrix debonding, as well as the effect of the size of the cluster of broken fibres on the stress recovery length.

2. Model description

2.1. Model geometry and failure process

Figure 1 shows a schematic representation of the bundle model used in this work. The bundle is formed by n_f fibres of length L arranged in a square packing. Each fibre is divided in n_{el} shorter elements, and therefore the bundle itself can be divided in n_{el} 2D cross-sections with n_f elements each. Each fibre element in the bundle is assigned a stochastic value of strength following a Weibull distribution.

The model is loaded by changing the value of the asymptotic stress σ_∞ applied at the extremities of the bundle. The value of σ_∞ is initially set to fail the weakest element in the bundle, and then progressively adjusted to cause more element failures. At each change in the value of σ_∞, the internal stress field in the bundle is re-computed considering the current configuration of broken elements in order to determine the next element that is due to break. When the number of broken elements is such that the surviving fibres are not able to withstand the total load, the bundle is considered failed and the bundle strength is taken as the the maximum value of asymptotic stress during the simulation.

A Monte Carlo study is used to determine the statistical distribution of the bundle strength: multiple simulations are carried out over different realisations of the elements strength assignment. The resulting values of bundle strengths can be analysed to determine the parameters of the statistical distribution.

Excerpt from ISBN 978-3-00-053387-7

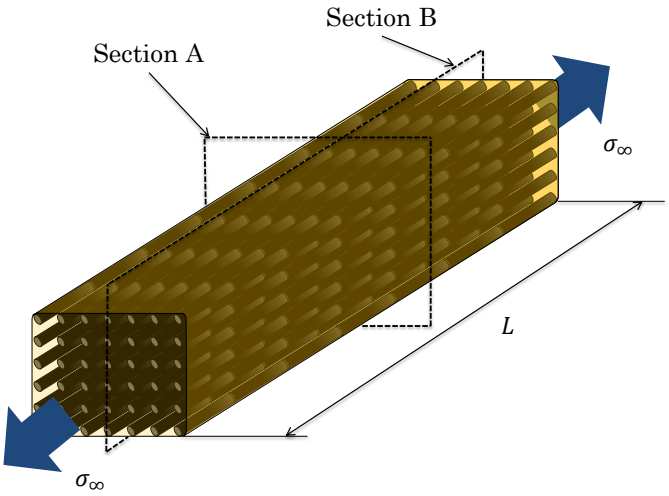

Figure 1: Schematic representation of the Fibre Bundle Model used in this study.

2.2. Stress recovery: shear-lag formulation

Given a particular configuration of broken elements and an assigned value of σ_∞, the internal stress field in the bundle is computed by first calculating the stress recovery along the fibres with a broken element j. In the vicinity of the fibre break, the tensile stress in the broken fibre at the longitudinal coordinate z can be determined using an analytical shear-lag function (Figure 2):

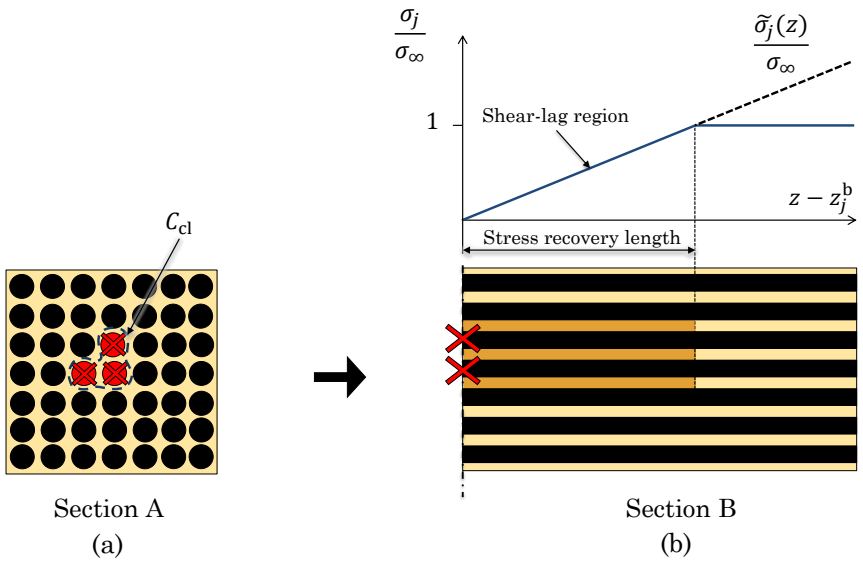

Figure 2: (a) Schematic representation of the bundle 2D cross section with three broken elements. (b) Shear-lag function used to calculate the stress recovery along the fibres with broken elements. The shear-lag function can account for the effects of fibre-matrix debonding and of the size of the clusters of broken fibres on the stress recovery length.

Excerpt from ISBN 978-3-00-053387-7

$$\tilde{\sigma}_j(z) = \frac{\tau \cdot C_j^{\mathrm{eq}}}{A_{\mathrm{f}}} \cdot (|z - z_j^{\mathrm{b}}|), \tag{1}$$

where j is the index of the broken elements in the bundle, C_j^{eq} is the equivalent shear-lag perimeter of the fibre, A_{f} is the fibre cross sectional area, and z_j^{b} is the longitudinal coordinate of the broken element.

The value of the shear stress τ can be set equal to the yielding strength of the matrix τ_{y} or to the interface friction stress τ_{fs}. Using this method, the effects of matrix yielding versus fibre-matrix debonding can be investigated.

The stress recovery length ℓ_{r} also changes with the size of the cluster of broken fibres. Larger clusters have a lower ratio of lateral surface over number of fibres in the cluster, and therefore fibres in larger clusters tend to have a longer recovery length. In the present model, this effect can be modelled by setting the equivalent shear-lag perimeter $C_{\mathrm{j}}^{\mathrm{eq}}$ equal to $C_{\mathrm{cl}}/n_{\mathrm{cl}}$, where C_{cl} is the perimeter of the cluster of broken fibres and n_{cl} is the number of fibres in the cluster. When neglecting this effect, the equivalent shear-lag perimeter $C_{\mathrm{j}}^{\mathrm{eq}}$ is set equal to the fibre circumference C^{f} regardless of the size of the broken cluster.

2.3. Stress redistribution: analytical power-law

After the longitudinal stress recovery in the fibres with broken elements has been calculated through shear-lag Section 2.2, the difference between the asymptotic stress and the local value of stress in the shear-lag region is redistributed over the intact elements in each 2D section of the bundle using an analytical power-law with an adjustable γ parameter. Hidalgo et al. [10] originally used a power-law with an adjustable γ parameter to calculate the stress concentration in a 2D fibre bundle model. In this work, their approach is expanded upon to adapt the formulation of the power-law to a full 3D bundle model and to account for the stress recovery along the fibre direction. The stress in each un-broken element of the bundle section (see Figure 3) can be calculated as

$$\begin{cases} \sigma_i(z) &= \sigma_\infty \cdot + \sum\limits_{j \in \mathrm{B}} K_j \cdot r_{ij}^{-\gamma}; \\ \\ K_j &= \left(\sigma_\infty - \sigma_{\mathrm{j}}(z)\right) \cdot \left(\sum\limits_{i \in \mathrm{I}} \mathrm{r}_{ij}^{-\gamma}\right)^{(-1)}; \end{cases} \tag{2}$$

where i is the index of the intact elements in the bundle, $\boldsymbol{I}$ is set of intact elements in the bundle 2D section, $\boldsymbol{B}$ is the set of broken elements in the bundle 2D section, and r_{ij} is the distance between the center of the broken element j and the intact element i. The appropriate value of γ for each material system is determined using FEA [15] (unlike in Hidalgo's approach, where γ was a free parameter of the model).

3. Results

Figure 4 shows a comparison of the experimental results on composite micro-bundles strengths reported by Beyerlein and Phoenix [2], versus predictions obtained with the present model for the same material systems. Beyerlein and Phoenix tested two different batches of four-fibres bundles to obtain statistical strength distributions. The fibre type was the same for both batches, but two different types of epoxy resin were used: a high modulus resin (Epoxy No. 1), and a low modulus resin (Epoxy No. 6). The

Excerpt from ISBN 978-3-00-053387-7

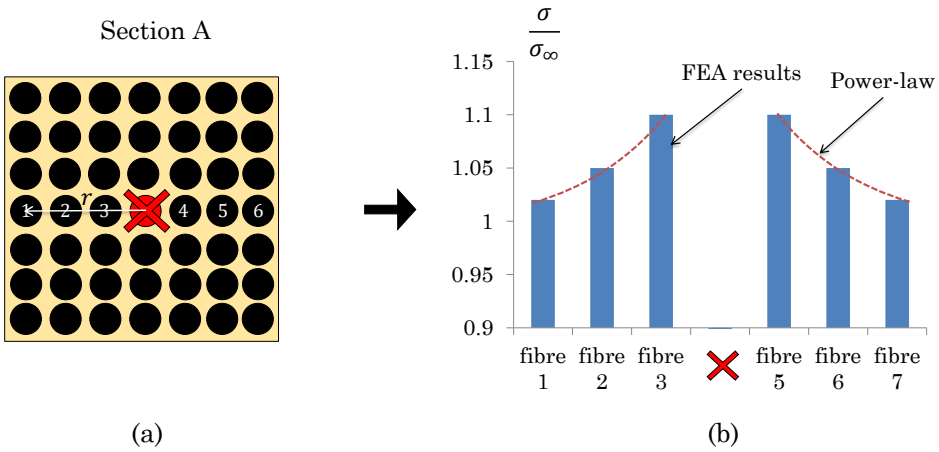

Figure 3: (a) Schematic representation of the bundle 2D cross section with one broken element. (b) Tensile stress in the surviving fibre elements in the bundle as determined by FEA [15], and approximated with the power-law function with parameter γ.

interfacial shear strength of these two resins was previously studied by Netravali et al [14], who noticed how Epoxy No. 1 showed fibre matrix debonding during single fibre fragmentation tests, while Epoxy No. 6 did not.

For the micro-bundles with Epoxy No. 1, the model predictions obtained considering perfect adhesion of the interface and yielding of the matrix (τ_y = 41.6 MPa) lead to an overestimation of the bundle strength (Figure 4(a)); considering friction after fibre-matrix debonding (τ_{fs} = 10 MPa) led to a good correlation with the experimental results (Figure 4(b)). For Epoxy No. 6, the model predictions obtained considering perfect adhesion of the interface and yielding of the matrix (τ_y = 3.96 MPa) are in very good agreement with the experimental results. The case of fibre-matrix debonding was not simulated for Epoxy No. 6 because was not observed experimentally. The full statistical distribution of strength for the four-fibres bundles was generated by the present model in under two minutes.

Figure 5 shows a comparison of experimental results on large composites bundles reported by Okabe and Takeda [3], versus strength predictions obtained with the present model. In this case, a bundle of 400 fibres was directly simulated with the model and the results have been scaled to larger bundle sizes using the Weakest Link Theory. The Monte Carlo study to obtain the average bundle strength and standard deviation for a bundle of 400 fibres was carried out by the present model in under two hours. Our model, accounting for fibre-matrix debonding (τ_{fs} = 10 MPa), and taking into account that the recovery length increases for larger cluster sizes, allows to explain the experimental results. Considering perfect adhesion of the interface and yielding of the matrix (τ_y = 52.4 MPa) would have led to a severe overestimation of the bundle strength. Finally, neglecting the variation in recovery length with the size of the cluster of broken fibres would have led to overestimating the bundle strength as well.

4. Discussion

The results shown in Figure 4 demonstrate how the present model is able to correctly predict the statistical distribution of strength for micro-bundles of four fibre with two different resin systems. For the high modulus resin, debonding was observed experimentally and the most accurate model predictions are

Excerpt from ISBN 978-3-00-053387-7

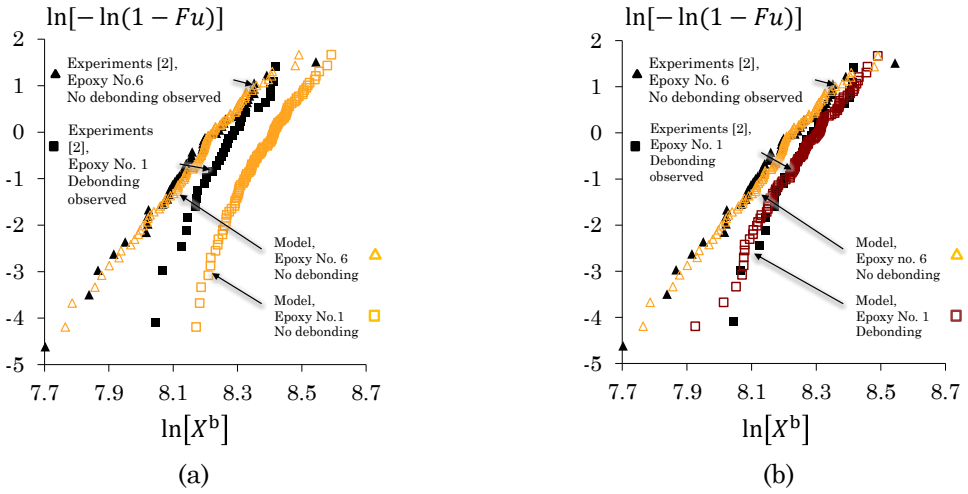

Figure 4: Failure probability F_u versus bundle strength X^b for two sets of micro-bundle of four fibres with different resin types. Experimental results from Beyerlein and Phoenix [2] are compared directly with the model predictions: (a) without considering debonding when observed experimentally; (b)with debonding when observed experimentally.

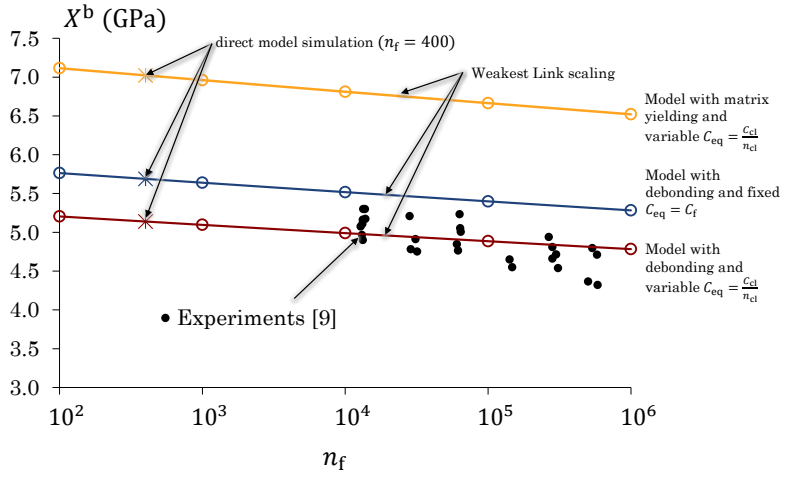

Figure 5: Average bundle strength X^b_{avg} versus number of fibres in the bundle n_f. Experimental results from Okabe and Takeda [3] are compared with model predictions scaled using Weakest Link Theory (WLT).

obtained when this effect is included in the model; neglecting it leads to strength overestimation. For the low modulus resin, debonding was not observed during experiments and accurate predictions are obtained when an intact fibre-matrix interface is considered in the model.

This effect is simulated in the present model by setting the value of the shear stress τ in the shear-lag calculations to be equal to the interface friction stress τ_{fs}, rather than the yielding strength of the matrix τ_y. This determines a longer recovery length ℓ_r and, therefore, a larger region of the bundle affected by the stress concentration. As a consequence, the probability of finding a weak fibre element inside the

Excerpt from ISBN 978-3-00-053387-7

stress recovery length increases and the average bundle strength tends to decreases. The effect of the size of the cluster of broken fibres on the recovery length is not significant for a bundle of four fibre; thus it was not discussed for the set of experiments in Figure 4.

Figure 5 demonstrates how the current model is able to correctly predict the average bundle strength for large bundles when the effects of fibre-matrix debonding (using τ_{fs} instead of τ_y) and the size of the cluster of broken fibres on the stress recovery length are taken into account. Neglecting them consistently led to an overestimation of the bundle strength.

Larger clusters have a smaller ratio of later surface to cross-section and this leads to a longer recovery length and therefore lower bundle strength. This effect is included in the shear-lag model by adjusting the equivalent shear-lag perimeter C_{eq}. Smaller values of C_{eq} result in longer recovery lengths which, in turn, result in a lower average bundle strength.

5. Conclusions

This paper presents a three-dimensional Fibre Bundle Model (FBM) to simulate the longitudinal tensile failure and predict the statistical strength distribution of CFRP bundles of different sizes. The model uses a semi-analytical approach to determine the stress field inside the bundle, and to predict the evolution of the failure process. A power-law is used to compute the in-plane stress redistribution due to one or multiple broken fibres, while the stress recovery along the broken fibres is computed using a shear-lag function. This accounts for the effects of matrix yielding and fibre-matrix debonding (by using the correspondent shear stress in the analysis), and of the size of the cluster of broken fibres on the stress recovery length (by accounting for the smaller equivalent perimeter of fibres in large clusters). The model results shown in Figure 4 and in Figure 5 compared favourably with different sets of experimental results, obtained for different fibre-matrix systems and different bundle sizes. The following conclusions can be reached:

- the modelling approach based on an analytical power-law and shear-lag functions appears to be suitable to correctly capture the most important aspects of the failure process of CFRP bundles under longitudinal tensile load;
- fibre-matrix debonding strongly influences the stress recovery length in broken fibres. In the present model, this effect can be included by setting the shear stress in the shear-lag function to be equal to the friction stress τ_{fs}. Neglecting this effect, when experimentally reported for the material system at hand, leads to an overestimate of the bundle strength;
- the stress recovery length for fibres with broken elements also depends on the size of the cluster of broken fibres. Accounting for this effect in the present model is important to correctly predict the experimental results. Neglecting this effect leads to an overestimation of the bundle strength;
- the present model gives full field data on the evolution of the failure process, while retaining computational efficiency due to its semi-analytical formulation. It is therefore suitable to be used to investigate the performance of different matrix-resin systems, and for micro-structure design and optimisation.

Acknowledgements

The first two authors are grateful to the funding from EPSRC under grant EP/M002500/1. The third author acknowledges the support from the Royal Academy of Engineering for her Research Fellowship on

Excerpt from ISBN 978-3-00-053387-7

Multiscale discontinuous composites for large scale and sustainable structural applications (2015/2019).

References

[1] H. E. Daniels. The statistical theory of the strength of bundles of threads I. *Mathematical and Physical Sciences*, 183:405–435, 1945.

[2] I.J. Beyerlein and S.L. Phoenix. Statistics for the strength and size effects of microcomposites with four carbon fibers in epoxy resin. *Composites Science and Technology*, 56(1):75–92, 1996.

[3] T. Okabe and N. Takeda. Size effect on tensile strength of unidirectional CFRP composites experiment and simulation. *Composites Science and Technology*, 62(15):2053–2064, 2002.

[4] C.M. Landis, I.J. Beyerlein, and R.M. McMeeking. Micromechanical simulation of the failure of fiber reinforced composites. *Journal of the Mechanics and Physics of Solids*, 48(3):621–648, 2000.

[5] S.J. Zhou and W.A. Curtin. Failure of fiber composites: A lattice green function model. *Acta Metallurgica Et Materialia*, 43(8):3093–3104, 1995.

[6] S. Mahesh, S.L. Phoenix, and I.J. Beyerlein. Strength distributions and size effects for 2D and 3D composites with weibull fibers in an elastic matrix. *International Journal of Fracture*, 115(1):41–85, 2002.

[7] T. Okabe, N. Takeda, Y. Kamoshida, M. Shimizu, and W.A. Curtin. A 3D shear-lag model considering micro-damage and statistical strength prediction of unidirectional fiber-reinforced composites. *Composites Science and Technology*, 61(12):1773–1787, 2001.

[8] Z.H. Xia and W.A. Curtin. Multiscale modeling of damage and failure in aluminum-matrix composites. *Composites Science and Technology*, 61(15):2247–2257, 2001.

[9] Z. Xia, W.A. Curtin, and T. Okabe. Green's function vs. shear-lag models of damage and failure in fiber composites. *Composites Science and Technology*, 62(10-11):1279–1288, 2002.

[10] R.C. Hidalgo, Y. Moreno, F. Kun, and H.J. Herrmann. Fracture model with variable range of interaction. *Physical Review E - Statistical, Nonlinear, and Soft Matter Physics*, 65(4):046148/1–046148/8, 2002.

[11] T. Okabe, H. Sekine, K. Ishii, M. Nishikawa, and N. Takeda. Numerical method for failure simulation of unidirectional fiber-reinforced composites with spring element model. *Composites Science and Technology*, 65(6):921–933, 2005.

[12] Y. Swolfs, R.M. McMeeking, I. Verpoest, and L. Gorbatikh. Matrix cracks around fibre breaks and their effect on stress redistribution and failure development in unidirectional composites. *Composites Science and Technology*, 108:16–22, 2015.

[13] S. Pimenta and S.T. Pinho. Hierarchical scaling law for the strength of composite fibre bundles. *Journal of the Mechanics and Physics of Solids*, 61(6):1337–1356, 2013.

[14] A.N. Netravali, R.B. Henstenburg, S.L. Phoenix, and P. Schwartz. Interfacial shear strength studies using the single-filament-composite test. I: Experiments on graphite fibers in epoxy. *Polymer Composites*, 10(4):226–241, 1989.

[15] L. St-Pierre and S.T. Pinho. Stress redistribution around broken fibres and strength of fibre bundles. *Abstract submitted to this conference*, 2015.

Excerpt from ISBN 978-3-00-053387-7